Thermotropic Biaxial Nematic Liquid Crystals

L. A. Madsen, T. J. Dingemans,* M. Nakata,† and E. T. Samulski
Department of Chemistry, University of North Carolina, Chapel Hill, North Carolina 27599-3290, USA
(Received 14 July 2003; published 9 April 2004)

We have synthesized liquid crystal (LC) mesogens based on a nonlinear oxadiazole unit that exhibit nematic phases near 200 °C. Polarized microscopy and conoscopy indicate that these LCs are biaxial nematics. Unambiguous and quantitative evidence for biaxiality is achieved using ^{2}H NMR spectroscopy. "2D powder" spectra, obtained by rotating ^{2}H-labeled samples about an axis perpendicular to the magnetic field at ~200 Hz, yield phase biaxiality parameters of ~0.1 when coupled with rigorous and proven simulations.

DOI: 10.1103/PhysRevLett.92.145505 PACS numbers: 61.30.Gd, 61.30.Eb

The biaxial nematic phase has eluded experimentalists since Freiser first hypothesized its existence in 1970 [1]. Theorists, on the other hand, were readily able to corroborate Freiser's predictions using a variety of methods [2,3]. Here we demonstrate experimentally that nematics composed of nonlinear boomerang-shaped molecules exhibit biaxial symmetry. The symmetry of long range orientational order in nematics, uniaxial ($D_{\infty h}$) or biaxial (D_{2h}), derives from molecular shape considerations. Anisometric molecular shape results in anisotropic excluded volume interactions, which propagate over mesoscopic scales in melts—the signature of thermotropic liquid crystals (LCs). Molecular analogs of extreme shapes, e.g., rodlike and disklike shapes [Figs. 1(a) and 1(b)], exhibit uniaxial nematic phases (N_u) in which their respective directors (axes of symmetry, $\boldsymbol{n}$) align in electric (magnetic) fields due to permittivity (susceptibility) anisotropies thereby generating the electro-optic response of the ubiquitous LC display.

In mixtures of rods and disks, the competition between the excluded volumes of the two different shapes results in a concentration regime wherein the rods and disks are oriented along mutually perpendicular major and minor directors, $\boldsymbol{n}$ and $\boldsymbol{m}$ [Fig. 1(c)], to form a biaxial nematic phase (N_b) [4,5]. This situation has been realized experimentally in a limited concentration range of complex aqueous mixtures of surfactants and alcohols, which form both rod- and disklike aggregates [6]. However, efforts to observe a N_b phase in two component melts of rod- and disklike LCs have been unsuccessful[5,7,8]. Even extravagant molecular architectures—covalently bonded disk and rod mesogens—have failed to exhibit the N_b phase [9]. For a single-component fluid comprised of parallelepipeds with sufficiently large aspect ratios [Fig. 1(d)], early theoretical studies predicted the N_b phase [2,3,10] and recent simulations [11] have borne this out. But while most calamitic LC molecules approximate a parallelepiped, to date there is only ambiguous and qualitative optical evidence for the existence of thermotropic N_b phases [12,13]. Recently, simulations on boomerang-shaped molecules (inset Fig. 1) concluded that N_b phases [Fig. 1(e)] are stable [14]. In our study we used boomerang-shaped mesogens derived from a 2,5-bis-(*p*-hydroxyphenyl)-1,3,4-oxadiazole (ODBP) core (Fig. 2) [16].

We were motivated to look for biaxial nematic phases in these boomerang-shaped mesogens because a related LC exhibited a "McMillan phase," a biaxial molecular arrangement in an orthogonal smectic *A* phase [17]. Additionally, the schlieren texture in the nematic phase of ODBP-Ph-C_7 was dominated by two-brush disclinations [16], equivocal evidence [18] of a N_b phase [19–21]. And recently, Acharya *et al.* reported [22] that the atypical four-spot x-ray diffraction patterns observed in the ODBP nematic phase and its *E*-field dependence could be

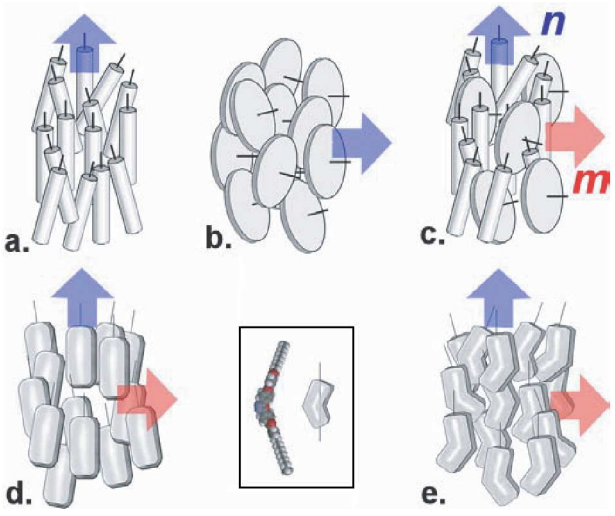

FIG. 1 (color online). Schematic illustration of nematic phases with major $\boldsymbol{n}$ and minor $\boldsymbol{m}$ directors: (a) uniaxial nematic comprised of cylindrically symmetric (calamitic) mesogens; (b) uniaxial (discotic) nematic; (c) biaxial nematic formed by a mixture of rods and disks; (d) biaxial nematic formed from anisometric parallelepiped platelets; (e) biaxial nematic phase of nonlinear (bent-core) mesogens. The inset shows the van der Waals surface of an ODBP mesogen and its boomerang abstraction.

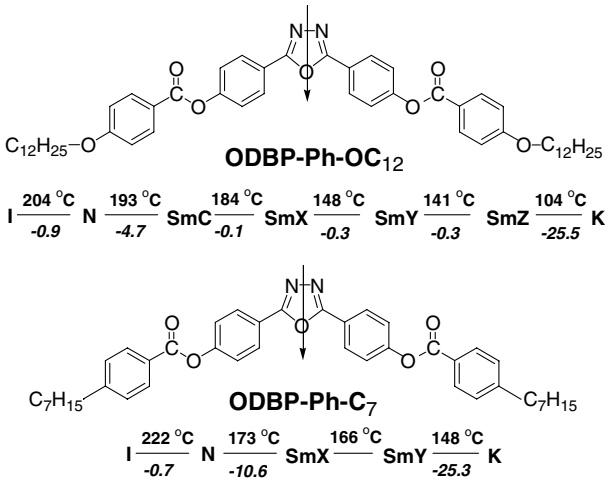

FIG. 2. Molecular structures and transition maps of two boomerang-shaped liquid crystals. The bisector of the bent (~140°) mesogenic core (oxadiazole) is coincident with the large (~4D), transverse electrostatic dipole moment [15].

reconciled only by modeling based on the bent molecule's form factor in conjunction with a N_b structure factor.

When we examined the nematic phases of both ODBP-Ph-OC_{12} and ODBP-Ph-C_7 with polarized microscopy using cells with a homeotropic surface treatment, we observed a birefringent schlieren texture [Fig. 3(a)]. This is not definitive evidence for a N_b phase as nonuniform director configurations ("chair" or "splay" distributions) in a uniaxial phase would also exhibit birefringence. However, "dark states"(quasi-isotropic domains) appear in homeotropic surface-treated wedge cells [Fig. 3(b)] and conventional cells at a cell thickness of 30 and 40 μm, respectively, for ODBP-Ph-OC_{12} and ODBP-Ph-C_7. Upon cooling the nematic, the birefringence of the dark state increased and conoscopy revealed a transformation from an apparent uniaxial structure to an increasingly biaxial structure [Fig. 3(c)]. If we assume that the phase is in fact uniaxial, the conoscopy would imply transitioning from a uniform homeotropic orientation to a gradient orientation [18], a higher distortion energy state. On the other hand, for a nonuniform director distribution in a biaxial phase, for example, a splay- or a bend-director configuration from the top to the bottom of the cell—an apparent, quasi-isotropic, dark-state texture would be achieved only at a certain temperature and cell thickness since normally the surface anchoring strength and the elastic constants would change with temperature. Hence, the evolution of the conoscopy indicates a change in anchoring and/or elasticity of a biaxial phase.

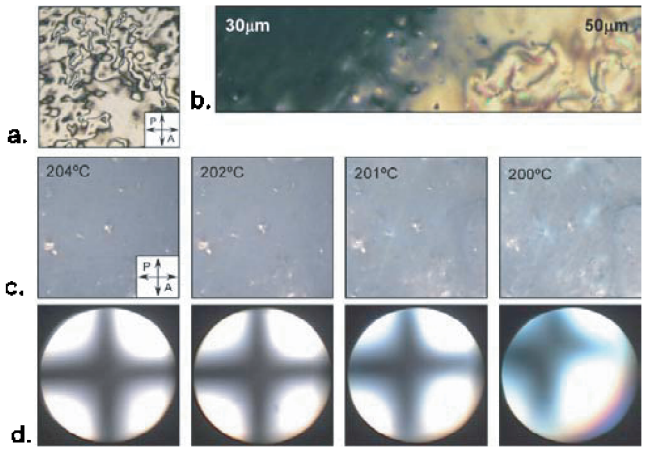

FIG. 3 (color online). Microscopy in the nematic phase of ODBP-Ph-OC_{12}. (a) Homeotropic 4 μm cell; (b) wedge-shaped cell with homeotropic surface treatment; (c) evolution of the birefringence of the "dark state" on cooling; (d) opening of the isogyres on cooling the dark nematic domain in (b).

While the optical data are strong evidence of a biaxial nematic phase in the ODBP mesogens, the caveat of surface-induced biaxiality cannot be ruled out [12]. We have focused on NMR, an inherently insensitive technique necessitating the use of bulk samples in which wall orientation effects are negligible. Moreover, in all previous claims where biaxiality was indicated by other methods, NMR experiments failed to corroborate it [23].

Phase biaxiality ($Q_{XX} \neq Q_{YY}$, where $\boldsymbol{Q}$ is any general, traceless, second rank tensorial property of the phase) is accessible only by NMR when the phase is interrogated along two axes of a phase-fixed X, Y, Z frame. This is a challenging undertaking in a nematic LC as the diamagnetic anisotropy $\Delta\chi = \chi_{ZZ} - 1/2(\chi_{XX+}\chi_{YY})$ anchors the primary director $\boldsymbol{n}$ (Z axis) along the spectrometer magnetic field $\mathbf{B}_0$. In this static case, the NMR spectrum of a ^{2}H-labeled mesogen exhibits a pair of lines split by ν_Q (in Hz), where ν_Q is proportional to the nuclear quadrupole tensor component q_{ZZ}, the motionally averaged component of the partially averaged quadrupole tensor $\boldsymbol{q}$ parallel to the major director $\boldsymbol{n}$; q_{XX} and q_{YY} are the components perpendicular to $\boldsymbol{n}$ [23,24]. These components determine the biaxiality parameter, $\eta = (q_{XX} - q_{YY})/q_{ZZ}$. Others have obtained the phase biaxiality in ^{2}H-labeled tilted smectics by rotating the sample and analyzing the resulting spectra using a detailed formalism [25,26].

By rotating the sample about an axis normal to $\mathbf{B}_0$ and above a critical rotation rate ω_C, the major directors $\boldsymbol{n}$ of subdomains of the sample become isotropically distributed in the plane perpendicular to the rotation axis. Under rotation, $\boldsymbol{n}$ experiences a torque of alignment toward $\mathbf{B}_0$, but is also dragged by the viscous torque of rotation. The NMR spectrum thus exhibits the two-dimensional (2D) "powder" pattern—a weighted average of the quadrupole spectra for a planar distribution of $\boldsymbol{n}$. A further alignment occurs for a biaxial LC with a magnetic susceptibility tensor ($|\chi_{ZZ}| < |\chi_{YY}| < |\chi_{XX}|$) such that the Y and Z components are uniformly distributed in the plane normal to the rotation axis and X aligns along that axis in order to minimize the magnetic free energy.

We followed the general methods of Goldfarb *et al.* [27] and Fan *et al.* [24] to calculate the 2D powder pattern. A component of the major director $\boldsymbol{n}$ makes an

angle θ with $\mathbf{B}_0$, and the transition frequency ν' of a given NMR line as a function of θ is given by

$$\nu'(\theta) = \nu_0 \pm (1/4)\nu_Q[(3\cos^2\theta - 1) + (1/2)\eta\sin^2\theta], \quad (1)$$

where ν_0 is the ^{2}H Larmor frequency including chemical shift. The 2D powder spectrum $S(\nu)$ is then calculated as an integral over Lorentzian lines with

$$S(\nu) = \frac{1}{\pi}\int_0^{2\pi} \frac{T_2}{\{1 + 4\pi^2 T_2^2[\nu - \nu'(\theta)]^2\}} d\theta, \quad (2)$$

where T_2 is the spin-spin relaxation time. One fits the rotation (2D powder) spectrum using Eq. (2) and the measured ν_Q from the static spectrum to quantify η.

The viscosities of our LC phases were much lower than in previous studies [23,28], such that the ω_C necessary to generate a planar director distribution was 120 Hz for the nematic and 90 Hz for the smectic C of the ODBP-Ph-OC_{12} compound, and 210 Hz near the lower transition point of the nematic range in ODBP-Ph-C_7. These high rotation rates necessitated use of theory derived by Photinos *et al.* to include rotational averaging in the simulations [28]. Since Gaussian line shapes fit the static spectra best for the ODBP-Ph-C_7 study, we simulated their 2D powder patterns using the convolution of a Gaussian line shape function with the Photinos result,

$$S(\nu) = J[0, z]C[e^{-[(\nu-E)^2/2\sigma^2]} + e^{-[(\nu+E)^2/2\sigma^2]}] + \sum_{i=1}^{\infty} J[i, z]C[e^{-[(\nu-E+2\omega_S)^2/2\sigma^2]} + e^{-[(\nu-E-2\omega_S)^2/2\sigma^2]} + e^{-[(\nu+E+2\omega_S)^2/2\sigma^2]} + e^{-[(\nu+E-2\omega_S)^2/2\sigma^2]}], \quad (3)$$

where $E = \nu_Q(1 + \eta)/8$, $z = \nu_Q(3 - \eta)/16\omega_S$, C is an overall scale factor, ω_S is the rotation rate in Hz, and σ is the spectral line half-width in Hz.

Our experimental apparatus consists of a Bruker ^{2}H static solids probe (72 mm OD) modified to include a rotation stage as well as a high temperature oven, which we detail elsewhere [29]. Temperature spread over the sample at 200 °C is ~1 °C, and rotation rates up to 300 Hz are possible.

Initially we focused on the ODBP-Ph-OC_{12} mesogen, which we deuterated at two distinct sites (Fig. 2) [30]. Since η is derived from a sum of three order parameters [25], the orientation of the label (C-D bond) in the molecule dramatically influences the measured value of η in these experiments. In the labeled ODBP-Ph-OC_{12} mesogen the situation was further compounded by a CSA ~ 60 Hz for the aromatic ^{2}H labels. In spectra of ODBP-d_4-Ph-OC_{12}, labeled at the 3,5 positions on the inner phenyl rings, quadrupole splittings ($\nu_Q = 250$ to 970 Hz in the nematic) were close in magnitude to the chemical shift anisotropy (CSA) interactions due to the (average) orientation of the C-D bond in the molecule. This prevented reliable fits of the rotation spectra using current theories, which do not account for CSA. The mesogen with ^{2}H at the 3,5 positions on the outer phenyls (ODBP-Ph-d_4-OC_{12}) showed a larger ν_Q (6.6–10.5 kHz in the nematic), which allowed fits to extract values of η. Representative nematic (190 °C) and smectic C (178 °C) rotation spectra yielded $\eta = 0.02 \pm -0.02$ and $\eta = 0.07 \pm -0.02$, respectively. That even the tilted smectic phase showed such a small η emphasizes that η is highly dependent on the label location in the molecule, and we had chosen an unfavorable case to study.

ODBP-Ph-C_7 exhibited a wider nematic temperature range (Fig. 2) and optical properties similar to ODBP-Ph-OC_{12} (Fig. 3). Solute "probe" molecules such as hexamethylbenzene-d_{18} (HMB) will adopt the orientational symmetry of the solvent [23,31]. The addition of 1.5 ± 0.5 wt % HMB to ODBP-Ph-C_7 depressed the N-I transition temperature by 17 °C and the SmX-N transition by 5 °C. This system showed a ν_Q of 4.0–6.1 kHz in the static nematic spectra. HMB shows a known splitting pattern [32] due to small (<20 Hz) dipolar couplings, but this influence on the rotation spectra fits was negligible. Similarly, adding a $P_2[\cos(\theta)]$ dependence to a constant linewidth minimally affected the fits [25,26,28].

Figure 4 shows the unequivocally biaxial rotation spectrum for the ODBP-Ph-C_7/HMB solution near the SmX-N transition along with simulations and a nonlinear least-squares fit generated using MATHEMATICA 4.1. The data are 8k pulse-acquire scans taken at $T = 174$ °C and $\omega_S = 230 \pm 8$ Hz. We fit the static spectrum at 174 °C to extract the quadrupole splitting ($\nu_Q = 5980$ Hz) and center offset frequency and used these values to constrain the rotation spectra fits. Because of a temperature uncertainty of ±2 °C during spinning, the error induced in ν_Q outweighs errors computed in the fit and places an upper bound on our error in η. Thus we measured a biaxiality parameter $\eta = 0.11 \pm 0.02$ for the ODBP-Ph-C_7/HMB solution, shown in Fig. 4(b). Figures 4(a) and 4(c) show the same data plotted with simulations where $\eta = 0$ and $\eta = 0.22$, respectively. Because of the viscosity drop with T, higher rotation rates ω_S were required to generate 2D powders. Our apparatus allowed NMR experiments at up to 184 °C ($\omega_S = 260$ Hz), 16 °C above the smectic-N_b phase transition of ODBP-Ph-C_7, where we measured $\eta = 0.08$. As we employ an indirect (probe) measurement, the reported values of η represent a lower bound on the phase biaxiality of ODBP-Ph-C_7. The magnitude of the biaxial order parameter we find seems plausible, i.e., the calculations of Vanakaras *et al.* [33] show that η could be as high as 0.2 + .

Since the discovery of ferroelectric switching in stratified (smecticlike) phases of nonlinear bent-core mesogens by Niori *et al.* [34], intense experimental effort has

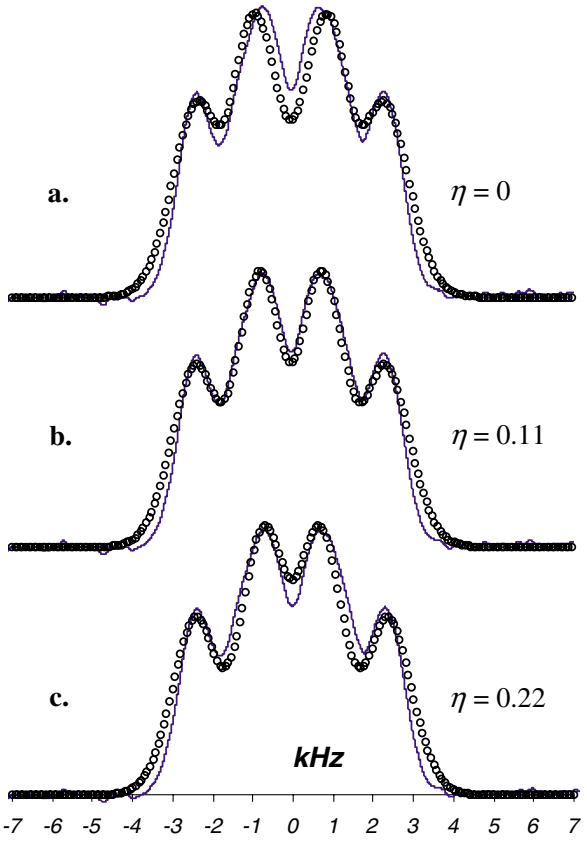

FIG. 4 (color online). NMR data and simulations for a rotating biaxial nematic. (a) Data on ODBP-Ph-C_7/HMB at 174 °C and rotating at 230 Hz (solid line) with the uniaxial simulation (circles); (b),(c) data with simulations where $\eta = 0.11$ (best fit) and $\eta = 0.22$.

focused on this class of so-called "banana" LCs. One striking discovery to accrue from this effort was that chiral LC phases could be spontaneously formed by achiral mesogens [35], a phenomenon anticipated by Freiser in his seminal paper [1]. But until now, unequivocal evidence for a biaxial nematic phase in a single-component thermotropic LC has eluded liquid crystallographers. The biaxial nematics reported here may originate from a delicate combination of excluded volume considerations coupled with electrostatic attraction: Although the nonlinearity of the ODBP core (~140° bend) is larger than that of the typical banana mesogens (~120° bend), and calamitic phases dominate the ODBP mesophases, ODBP boomerangs possess very biaxial shapes. But relative to conventional biaxial-shaped calamitic mesogens, ODBP boomerangs have the added possibility of strong intermolecular associations originating from the large electric dipole moment of the oxadiazole ring. Such associations are predicted to reinforce transverse orientational correlations driven by shape and thereby stabilize the N_b phase [33].

This research was supported by the National Science Foundation (DMR-9971143). The authors thank Alex Chao for assistance with NMR measurements and Demetri Photinos for helpful discussions.

*Permanent address: Fundamentals of Advanced Materials Group, University of Delft, 2629 HS Delft, The Netherlands.
†Permanent address: Department of Organic and Polymeric Materials, Tokyo Institute of Technology, Tokyo 152-8552, Japan.

[1] M. J. Freiser, Phys. Rev. Lett. **24**, 1041 (1970).
[2] C.-S. Shih and R. Alben, J. Chem. Phys. **57**, 3055 (1972).
[3] J. P. Straley, Phys. Rev. A **10**, 1881 (1974).
[4] A. Stroobants and H. N. W. Lekkerkerker, J. Phys. Chem. **88**, 3669 (1984).
[5] H. H. Wensink, G. J. Vroege, and H. N. W. Lekkerkerker, Phys. Rev. E **66**, 041704 (2002).
[6] L. J. Yu and A. Saupe, Phys. Rev. Lett. **45**, 1000 (1980).
[7] A. G. Vanakaras and D. J. Photinos, Mol. Cryst. Liq. Cryst.: Sci. Tech. A **299**, 65 (1997).
[8] S. Varga, A. Galindo, and G. Jackson, Phys. Rev. E **66**, 011707 (2002).
[9] J. J. Hunt *et al.*, J. Am. Chem. Soc. **123**, 10115 (2001).
[10] R. Alben, Phys. Rev. Lett. **30**, 778 (1973).
[11] R. Berardi and C. Zannoni, J. Chem. Phys. **113**, 5971 (2000).
[12] G. R. Luckhurst, Thin Solid Films **393**, 40 (2001).
[13] D. W. Bruce, G. R. Luckhurst, and D. J. Photinos, Mol. Cryst. Liq. Cryst. **323**, 153 (1998).
[14] P. I. C. Teixeira, A. J. Masters, and B. M. Mulder, Mol. Cryst. Liq. Cryst. **323**, 167 (1998).
[15] T. J. Dingemans, N. S. Murthy, and E. T. Samulski, J. Phys. Chem. B **105**, 8845 (2001).
[16] T. J. Dingemans and E. T. Samulski, Liq. Cryst. **27**, 131 (2000).
[17] K. J. K. Semmler, T. J. Dingemans, and E. T. Samulski, Liq. Cryst. **24**, 799 (1998).
[18] Y. Galerne, Mol. Cryst. Liq. Cryst. **311**, 211 (1998).
[19] S. Chandrasekhar *et al.*, Curr. Sci. **75**, 1042 (1998).
[20] S. Chandrasekhar *et al.*, Liq. Cryst. **24**, 67 (1998).
[21] C. Chiccoli *et al.*, Phys. Rev. E **66**, 039701(R) (2002).
[22] B. R. Acharya *et al.*, Pramana **61**, 231 (2003); reprinted in Phys. Rev. Lett. **92**, 145506 (2004).
[23] J. R. Hughes *et al.*, J. Chem. Phys. **107**, 9252 (1997).
[24] S. M. Fan *et al.*, Chem. Phys. Lett. **204**, 517 (1993).
[25] P. J. Collings *et al.*, Phys. Rev. Lett. **42**, 996 (1979).
[26] D. J. Photinos, P. J. Bos, and J. W. Doane, Phys. Rev. A **20**, 2203 (1979).
[27] D. Goldfarb *et al.*, J. Chem. Phys. **79**, 4035 (1983).
[28] D. J. Photinos and J. W. Doane, Mol. Cryst. Liq. Cryst. **76**, 159 (1981).
[29] L. A. Madsen and E. T. Samulski (to be published).
[30] T. J. Dingemans, L. A. Madsen, and E. T. Samulski (to be published).
[31] D. J. Photinos, in *NMR of Ordered Liquids*, edited by C. E. de Lange (Kluwer, Dordrecht, 2003).
[32] J. W. Emsley and J. C. Lindon, *NMR Spectroscopy Using Liquid Crystal Solvents* (Pergamon Press, Oxford, 1975).
[33] A. G. Vanakaras, A. F. Terzis, and D. J. Photinos, Mol. Cryst. Liq. Cryst. **362**, 67 (2001).
[34] T. Niori *et al.*, J. Mater. Chem. **6**, 1231 (1996).
[35] D. R. Link *et al.*, Science **278**, 1924 (1997).